Hindawi Publishing Corporation
Laser Chemistry
Volume 2009, Article ID 295765, 10 pages
doi:10.1155/2009/295765

Research Article

Development, Characterization, and Application of a Versatile Single Particle Detection Apparatus for Time-Integrated and Time-Resolved Fluorescence Measurements—Part I: Theoretical Considerations

Xihong Wu, N. Omenetto, and J. D. Winefordner

Department of Chemistry, University of Florida, Gainesville, FL 32611, USA

Correspondence should be addressed to N. Omenetto, omenetto@chem.ufl.edu

Received 31 January 2009; Accepted 27 March 2009

Recommended by Savas K. Georgiou

Recent progress in aerosol science has resulted in more challenging demands in the design of new particle beam introduction systems. In this paper, the concept of a variable orifice aerodynamic lens system is presented and supported by the numerical simulation results. This novel particle beam inlet can serve as either a narrow band pass filter (a particle segregator) that only confines particles with a specific size or a broad band pass filter (a particle concentrator) that allows particles with a wide size range to be concentrated on the beam axis. Following a brief description of the inlet system, computational details are described. Simulation of this inlet has been carried out by the commercial computational fluid dynamics protocol FLUENT. Focusing performance and characteristic of single-thin plate orifices have been first revealed and discussed, and then the dynamics and advantages of using multiple lenses with variable orifices are addressed. It is clearly shown that the focusing size range can be primarily adjusted by varying the working pressure, the orifice geometry, and/or the arrangement of orifices. As a result, a selection of the desired particle focusing size range can be achieved without the need of changing the inlet, thus increasing the versatility of the device for a broad range of applications.

1. Introduction

Rapid detection of ambient aerosols, especially bioaerosols, is inherently difficult due to the low concentration at which species are found. Laser-based detection methods are popular among modern aerosol measurement techniques. One of the major drawbacks hindering the application of laser spectroscopy in the single particle analysis scheme is the spatial misalignment between the well-confined, focused laser beam waist and the incoming dispersed, low concentration flow of particles. It is, therefore, highly desirable to confine the particles to the beam axis prior to analysis, thus increasing the probability of hitting them with a tightly focused laser beam. The most desirable particle inlet would be the one capable of forming a narrow particle beam on line in real time [1].

It is well known [see, e.g., [2–16]] that a particle beam can be formed when aerosols are expanded into a vacuum where the carrier gas is scattered away by intermolecular collisions and the seeded particles are accelerated and dragged into the central core of the jet due to their large momentum. It is not our intention here to provide a detailed review of the extensive literature existing on this topic: rather, reference will be given to only a few selected publications relevant to the work described in this paper. Although the considerations given below are well known and have been reported before, they are needed to follow the theoretical design of the apparatus developed in our laboratory.

Since the pioneer work of Murphy and Sears on the production of a particle beam using expansion through a capillary [2], extensive theoretical and experimental studies have been devoted to it [3–8]. It has been proven that particles cross a singular point after passing through a highly convergent nozzle such as a thin-plate orifice [9]. However, the beam diverges rapidly after the focal point, thus precluding the use of highly convergent nozzles when

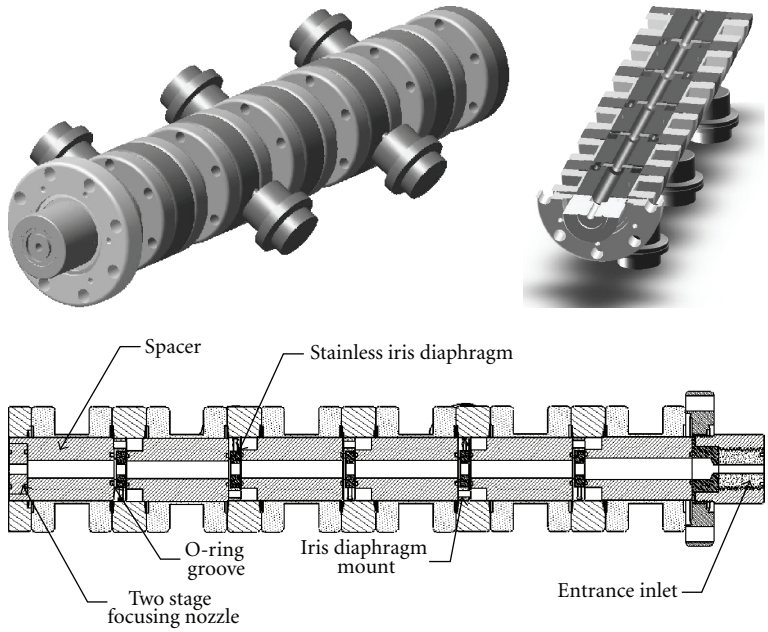

Figure 1: Layout of the variable-orifice aerodynamic inlet: 3D view (top); 2D section view (bottom).

measurements are made far away from the nozzle exit. Conversely, a particle beam formed with a slowly convergent nozzle (a capillary would be the limiting case) crosses the axis at a relatively longer distance. Therefore, the beam has a small expansion angle and can survive far away from the exit [10]. A particle beam with a solid angle as small as 10^{-4} sr was observed by Israel and Friedlander using a capillary at low pressure [3]. However, the disadvantage of using a capillary is that it becomes easily clogged. Theoretical studies carried out by Mallina et al. [11] have suggested that a single sharp orifice can efficiently transmit particles with a selected narrow size range under specific condition, although the working pressure needs to be scanned in order to aerodynamically focus, in a sequential way, particles over a wide size range. This type of particle beam inlet is referred to as a "segregator" in this study since it can only produce particle beam within a small size range window.

The most remarkable accomplishment in particle beam inlets comes from the development of the aerodynamic lenses which have the ability to confine particles over a wide size range using a series of concentric lenses with successively reduced diameters housed inside a tube. The first aerodynamic lens inlet designed by Liu et al. produced narrow beams for particles over a range of 40–250 nm without sheath air [12, 13]. Theoretical studies to evaluate the performance of aerodynamic inlets have been recently performed by several groups [12–16]. For example, particle motion through a single lens and multiple aerodynamic lenses was simulated by Zhang et al. [17], using FLUENT, a commercial computational fluid dynamics (CFD) software package, and the results indicated that the focusing characteristics strongly depend on the inlet geometry and working conditions. More recently, a detailed design guideline to focus particles as small as 5 nm using an aerodynamic lens system has been proposed [15, 16].

In our laboratory, the interest has been focused in recent years on the study of the interaction between particles and laser radiation with different experimental approaches, such as laser-induced fluorescence (LIF) and laser-induced breakdown spectroscopy (LIBS), with the aim of characterizing both biological and nonbiological particles and of developing a real-time sensing protocol involving both analytical techniques, in particular exploring the potential of time-resolved measurements [18, 19]. A wide range of particle diameters is expected, ranging from about 0.1 μm to several μm. Moreover, the residence time of the particle in the interaction volume should also be variable. The existing particle beam inlets have limited focusing size ranges. Switching between a concentrator (multidiameters) and a segregator (single diameter), as well as between different working conditions is difficult for the currently available multiple-lens aerodynamic inlets since their geometry is fixed, pressure being the only parameters that can be adjusted in order to optimize the particle focusing performance. Our solution to accomplish this challenge is to construct an inlet *with variable orifices* so that varying both pressure and geometry can dynamically alter the focusing size range. This inlet can also serve as either a concentrator or a segregator according to the application demands.

The work is divided in two parts: in this first paper, the theory underlying the design of a variable-orifice aerodynamic lens inlet that has the capability of size focusing range selection is presented. Numerical simulations are used to examine the performance of such a novel particle beam inlet. Simulation results provide the fundamental basis for the construction, evaluation, and optimization of

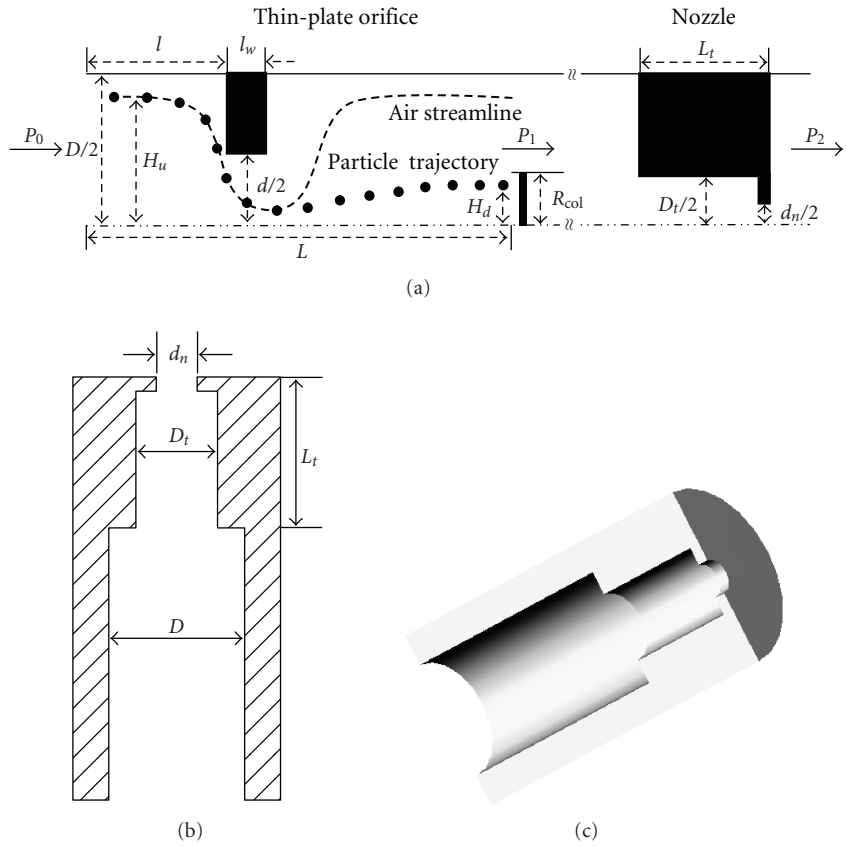

Figure 2: Sketch of an aerodynamic inlet including a thin-plate orifice and a two-stage nozzle [12, 13] (P_0, P_1 are the upstream and downstream pressure of the inlet, resp. P_2 is the downstream pressure of the focusing nozzle). H_u and H_d represent the particle initial and final radial positions. R_{col} is the radius of the detection area.

the variable orifice aerodynamic inlet. The technical and analytical characterization of this apparatus is described in detail in a companion paper [20].

2. System Description

The inlet used in our single particle detection system is composed of five variable orifices. The schematic of the inlet is displayed in Figure 1. Each aerodynamic lens is made of a stainless steel iris diaphragm (Edmund Industrial Optics). A pin located at the top of the iris can be rotated through 90 degrees to allow the iris aperture to be continuously varied from 0.8 mm to 8.5 mm. A high vacuum linear motion feed through controls the motion of the pin. All five lenses are mounted on flanges at a particular position with respect to axis of the shaft so that all lenses have the same opening of 8.5 cm when the micrometers read zero. Prior calibration of the micrometer reading versus aperture size is accomplished, thus allowing varying the aperture size without breaking the vacuum.

3. CFD Simulation Details

FLUENT 6.1.22 protocol is employed for all CFD calculations. For all flows of interest, three governing equations, that is, continuity, conservation of momentum, and conservation of energy are solved with FLUENT based on the finite volume method to obtain the flow field parameters [21]. Figure 2 shows the schematics of a single lens inlet employed in the numerical simulation, as well as the air streamline and particle trajectory. A typical two-stage nozzle is also included. The tube diameter (D) is set at 1.2 cm for all simulations, unless otherwise specified.

The thickness (l_w) of the lens is fixed at 0.3 mm, while the lens diameter (d_i) is adjusted for different D/d_i ratios. The inlet and its corresponding grid are generated by GAMBIT 2.1.6, a preprocessor bundled with FLUENT 6.1.22 protocol. The flow field is divided into submap domains possessing structured quadrilateral mesh. To eliminate the dependence of the simulation results on the grid density, the inlet is calculated with different mesh densities, and a settled grid density (axial—10 grid/mm, radial—16.7 grid/mm) is then chosen throughout the simulation. In addition, grid adaptation, based on the flow field velocity gradient after the initial iterations, is applied to enhance the computational accuracy. The mesh is subsequently introduced to the solver, and air (considered as ideal gas) is added to the flow field. A power-law model is used to estimate the variation of the viscosity with temperature. The convergence criteria are set to at least 10^{-6} for all iteration residuals. The flow

field ($T = 300\,\mathrm{K}$) is optimized with a segregated two-dimensional double-precision axi-symmetric solver. Finally, discretization is changed from first to second-order upwind to increase accuracy.

Once the flow field is established, spherical particles with a unity density of $1000\,\mathrm{kg/m^3}$ are. introduced into the solution domain. Three assumptions are made. First, all particles are inert, that is, no thermal energy is transferred through particle-particle or particle-fluid interaction. Second, particles are trapped without bouncing when colliding with walls of the tube or lenses. Finally, forces other than the drag force, such as Brownian diffusion, are neglected in the simulation. To improve the accuracy, Cunningham correction factors for all particles sizes are computed by a user-defined function based on the local temperature and pressure of the flow domain.

The particle trajectory is tracked by the discrete phase model *via* the Lagrangian method. With the assumption of free particle-particle and particle-fluid interaction, the motion of each particle based on the drag force is governed by

$$\frac{du_p}{dt} = \frac{u - u_p}{\tau}. \tag{1}$$

In (1), u and u_p are field and particle velocity, respectively, and τ is the particle relaxation time. For a spherical particle with a diameter of d_p, the dynamic properties are described by the particle Reynolds number (Re_p), Knudsen number (Kn), and Stokes number defined as follows:

$$\mathrm{Re_p} = \frac{\left|u - u_p\right|\rho d_p}{\mu}, \tag{2}$$

$$\mathrm{Kn} = \frac{2\lambda}{d_p}. \tag{3}$$

Here, λ (μm) is the mean free path of the air given as [22]

$$\lambda = 0.0665 \times \frac{101325}{p} \times \frac{T}{293.15} \times \frac{1 + 110/293.15}{1 + 110/T}. \tag{4}$$

If Re_p is less than 1, as in our case, particle relaxation time (s) is given by

$$\tau = \frac{\rho_p d_p^2 C_c}{18\mu}, \tag{5}$$

where the Cunningham slip correction C_c can be written as follows [23]:

$$C_c = 1 + \mathrm{Kn}\left(1.257 + 0.4e^{-1.1/\mathrm{Kn}}\right). \tag{6}$$

Technically, the Stokes number (Stk), a complex function of lens geometry, flow field and particle properties, is commonly accepted as a characteristic number to describe the particle dynamic motion in aerodynamic inlets:

$$\mathrm{Stk} = \frac{U}{d_i}\tau. \tag{7}$$

In this study, the Stokes number is calculated based on the parameters obtained at the orifice exit. The orifice diameter d_i is used as the characteristic length scale of the system and the average flow velocity at the lens exit is taken as the characteristic velocity U.

Assuming an operating temperature of 300 K and combining (3), (4), and (6), the Cunningham correction factor can be calculated by

$$C_c = 1 + \frac{a}{pd_p} \times \left(1.257 + 0.4e^{-1.1pd_p/a}\right) \quad (a = 0.014\ \mathrm{Pa \cdot m}). \tag{8}$$

Thus, the particle Stokes number can be rewritten as

$$\begin{aligned} \mathrm{Stk}(m) &= k \cdot C_c \cdot \left(pd_p\right)^2 \cdot \frac{1}{p^3} \cdot \frac{1}{d_i^3} \\ &= \frac{2}{9\pi} C_c \cdot \rho_p d_p^2 \cdot \frac{m}{\rho\mu} \cdot \frac{1}{d_i^3}, \end{aligned} \tag{9}$$

$$k = \frac{2}{9\pi}\frac{RT}{M} \cdot \frac{1}{\mu} \cdot \rho_p \cdot m. \tag{10}$$

As seen in (10), k is an important constant associated with the mass flow rate. The right hand side of (9) is the product of several terms, related to the correction factor, the particle properties (size and density), the flow field properties, and finally the effect of the lens geometry to the Stokes number. Clearly, the particle Stokes number indeed consists of all parameters that possibly affect the characteristics of particle focusing through thin-plate orifices. Consequently, the particle Stokes number determines the focusing characteristic through aerodynamic inlets. For any given orifice and operating condition, only particles with a specific size (optimal particle size, $d_{p,\mathrm{opt}}$) can be optimally collimated into the narrowest beam. The relevant Stokes number is referred as the *optimal* Stokes number.

4. Results and Discussions

4.1. Single Thin-Plate Orifice. A detailed understanding the focusing behavior of single lens not only provides guidance and insight into the analysis of multiple lenses, but also helps to optimize the working parameters and inlet geometry design with less CPU time. In literature, *contraction factor* η_{cf} (defined as the ratio of the particle final radial position H_d to initial radial position H_u as shown in Figure 2) [12] and *transmission efficiency* η_{te} (defined as the ratio of the particle downstream mass flow rate to the upstream flow rate) [17] have been used to evaluate the focusing capability of a single lens. However, it is more relevant to investigate the dependence of the *collimation efficiency* η_{ce} on the working conditions, since, in laser-based detection techniques, only particles located within the laser focal point can be detected. In this paper, the collimation efficiency is defined as the fraction of particles entering a detection area centered on the axis of the orifice exit plane. In most of the simulations, the detection area is set as an area with a diameter of 500 μm, the typical size of laser beam waist, and

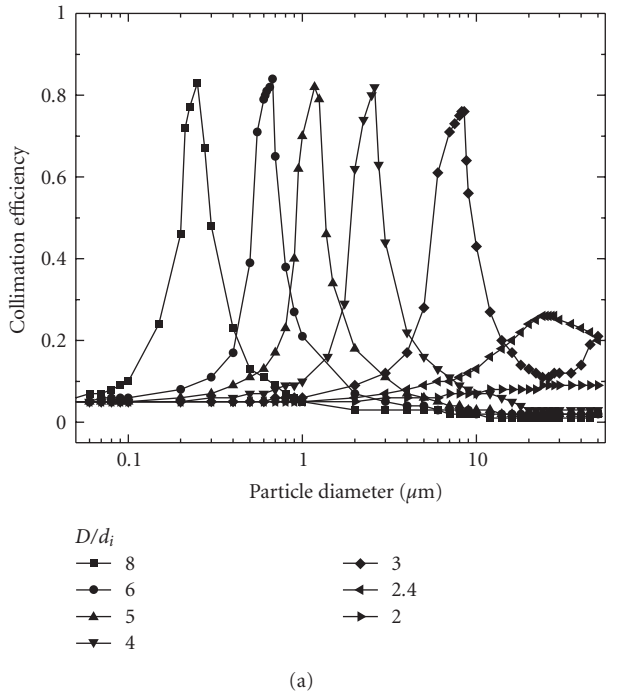

(a)

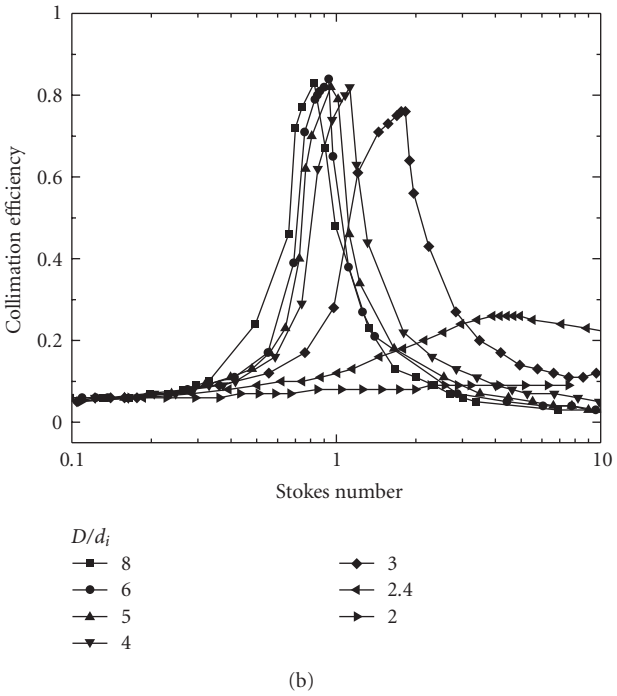

(b)

Figure 3: Effect of lens geometry on particle collimation efficiency for a thin-plate orifice: (a) η_{ce} versus d_p; (b) η_{ce} versus Stk at $D = 12$ mm, $P_0 = 1000$ Pa, and $Q = 60$ sccm.

is located at 5 cm downstream of the orifice, unless stated otherwise. Unlike the simulation carried out by Liu et al. [12], where only near-axis injection is considered, particles are uniformly injected through the whole inlet surface area when calculating the collimation efficiency. Clearly, the collimation efficiency is simultaneously associated with both the contraction factor and the transmission efficiency. The size of optimally transmitted particles with the narrowest beam width corresponds to the diameter of particles with either $\eta_{cf} = 0$ or the highest η_{te}.

Figure 3 illustrates the influence of the ratio of the tube diameter to that of the orifice diameter on the collimation efficiency at a flow rate (Q) of 60 sccm. The working pressure is kept fixed at 1000 Pa. It can be seen that the size of the optimal particle (the particle with the highest collimation efficiency) $d_{p,\text{opt}}$ strongly depends upon the lens diameter. Specifically, orifices with larger diameters optimally focus larger particles. However, for a lens with a diameter of 5 mm, the collimation efficiency for the optimal particles degrades remarkably and the curve is much broader. For $d = 6$ mm, no particle can be effectively accumulated within the detection area. When plotted *versus* the particle Stokes number in Figure 3(b), the collimation efficiency is nearly independent on lens geometry for aerodynamic inlets with a d/D ratio less than or equal to 1/4, and the optimal Stokes number is about one.

For higher d/D ratios, the curve is broadened and the optimal focusing takes place at a Stokes number greater than one.

As shown in Figure 4, the behavior of the collimation efficiency against particle size at different pressures with fixed lens dimension exhibits a similar distribution. At higher working pressures, the fluid introduces a larger drag force, and particles with a larger size (inertia) are required to achieve the optimal focusing. When examining the dependence of the collimation efficiency under different pressures on the Stokes number, it can be seen that all curves collapse into a single curve, as shown in Figure 4(b), indicating that the Stokes number does include the influence of pressure on the focusing performance of aerodynamic inlets. Additionally, the optimal Stokes number is close to one, varying from 0.8 to 1.1. The dependence of the optimal value of the Stokes number on the Mach number, Reynolds number, and lens geometry has been observed in previous studies [12, 17, 24].

For those particle injected near-axis, the optimal Stokes number changes from 0.7 to 1.1, while Reynolds numbers decrease from 500 to 10. It was also found that, as the Mach number decreases from 0.843 to 0.009, the optimal Stokes number increases from 0.55 to 0.8 [12].

Rearranging (9), the orifice diameter (d_i) capable of focusing any size (d_p) of particles under a desired working condition can in principle be determined from the relation:

$$d_i = \left\{ k \cdot \left[1 + \frac{a}{p d_p} \times \left(1.257 + 0.4 e^{-1.1 p d_p / a} \right) \right] \cdot \left(p d_p \right)^2 \cdot \frac{1}{p^3} \right\}^{1/3} \cdot \text{Stk}_{\text{opt}}^{1/3}. \tag{11}$$

The orifice diameter calculated from (11) by assuming the optimal Stokes number = 1 is plotted in Figure 5 as a function of particle size under different operating pressures. Note that fixing the optimal Stokes number to 1 could result in 16% error in predicting the orifice size. However, the

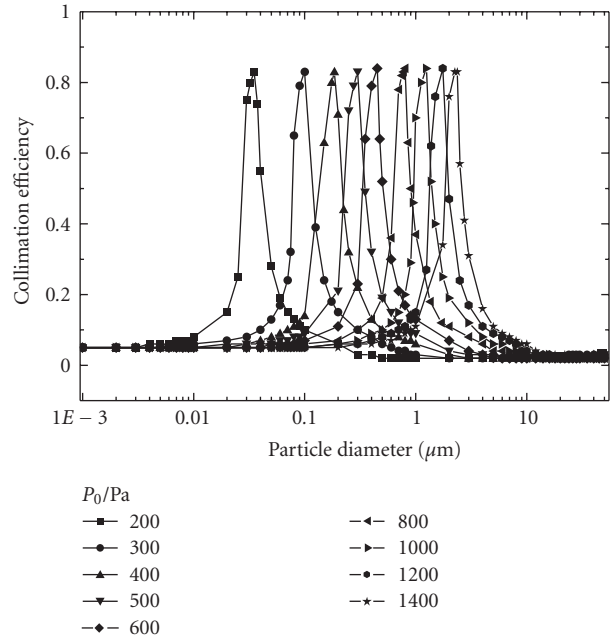

(a)

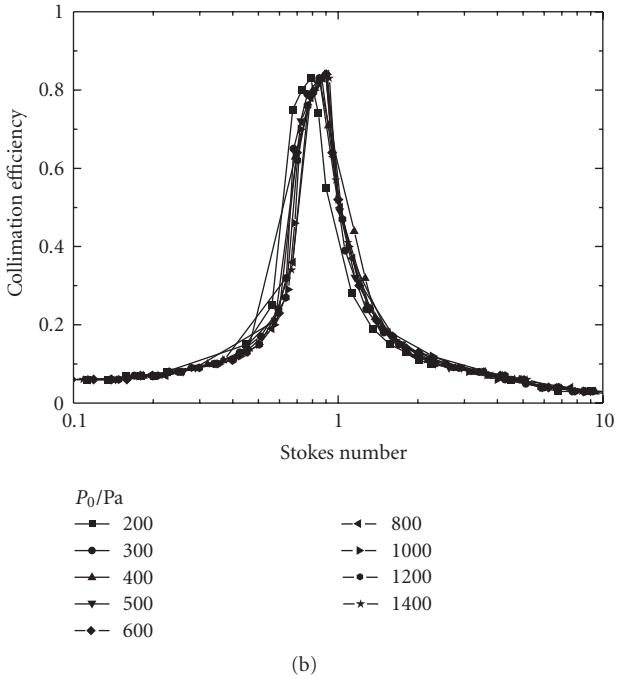

(b)

Figure 4: Effect of the operating pressure on particle collimation efficiency for a thin-plate orifice: (a) η_{ce} versus d_p; (b) η_{ce} versus Stk at $D = 12$ mm, $d_i = 2.4$ mm, and $Q = 60$ sccm.

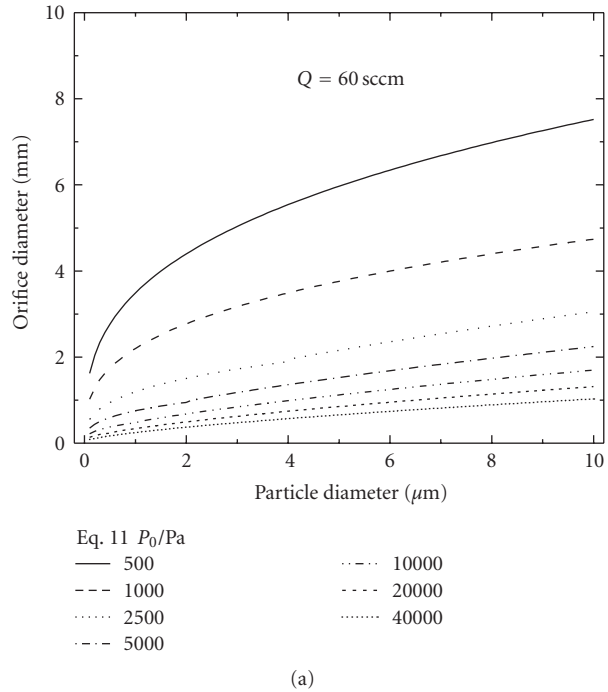

(a)

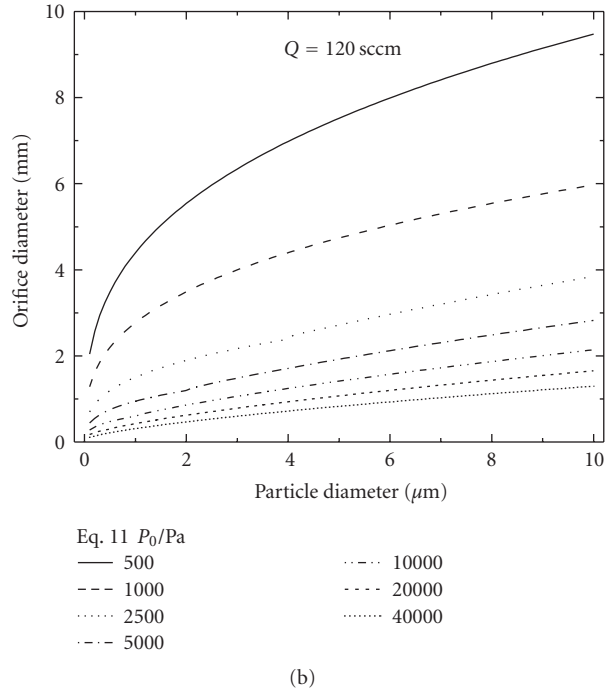

(b)

Figure 5: Predicted orifice diameter versus particle size under different upstream pressures at $Q = 60$ (a) or 120 sccm (b).

results reveal that particles with a specific size can be focused by either an inlet with a larger diameter at lower pressure or an inlet with a smaller aperture at higher working pressure, whereas at a certain pressure, a particle of a specific size can be focused by either a smaller orifice at a lower flow rate or a larger lens at a higher flow rate. For a given orifice, the particle size it can focus increases with an increase of the working pressure. However, it becomes less dependent on the pressure at higher working pressures. For example, As shown in Figure 5(b), for a orifice size of 1 mm as the pressure increases from 1×10^4 Pa to 4×10^4 Pa (a 4-fold increase), the optimal size increases by a factor of 2.4, while as the pressure changes from 1×10^4 Pa, to 2×10^4 Pa (a 2-fold increase), the optimal size increases by a factor of 1.6. On the other

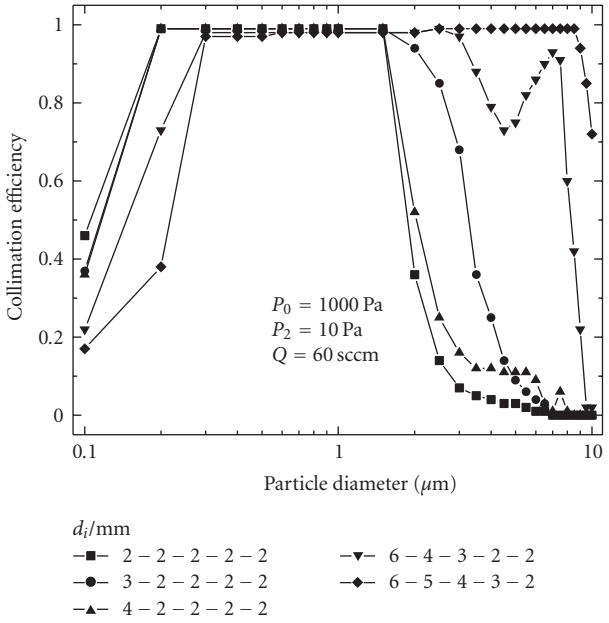

Figure 6: Dependence of the detection efficiency on the orifice geometry for aerodynamic inlets integrated with a two-stage nozzle (L_t = 10.0 mm; D_t = 2.0 mm; and d_n = 1.0 mm) under the same operating conditions at D = 12 mm.

hand, the orifice geometry has a stronger effect on particle focusing. The optimal particle size always increases with the lens diameter and the influence is even stronger at higher working pressures. A slight change in the lens diameter could result in a significant change in the optimal particle size at high pressure.

4.2. Multiple-Lens Particle Inlets with Variable Orifices. As discussed before, it is evident that a single lens can only confine particles with a particular size into a narrow beam. However, in those cases where simultaneous focusing of particles over a wide size range is desirable, multiple aerodynamic lenses have to be used. Our newly designed inlet is composed of five continuously variable orifices whose diameters are tunable from 0.8 to 8.5 mm. In theory, the orifice diameter can be set to any allowed value, and the resultant focusing size range is different from case to case. The advantage of such a system is that not only varying the working pressure but also the lens diameter can alter the focusing size range. As a result, arbitrary focusing size ranges can be chosen. In addition, this novel particle beam inlet can serve either as a narrow band pass filter (segregator) or broad band pass filter (concentrator) allowing particle with a selected size range to concentrate on the beam axis. Note that all the above attributes cannot be realized by simply varying the working pressure.

Figure 6 compares the detection efficiency measured 5 cm away from the nozzle exit for five different inlets ended with the same two-stage nozzle (L_t = 10.0 mm; D_t = 2.0 mm; d_n = 1.0 mm) under the same working conditions.

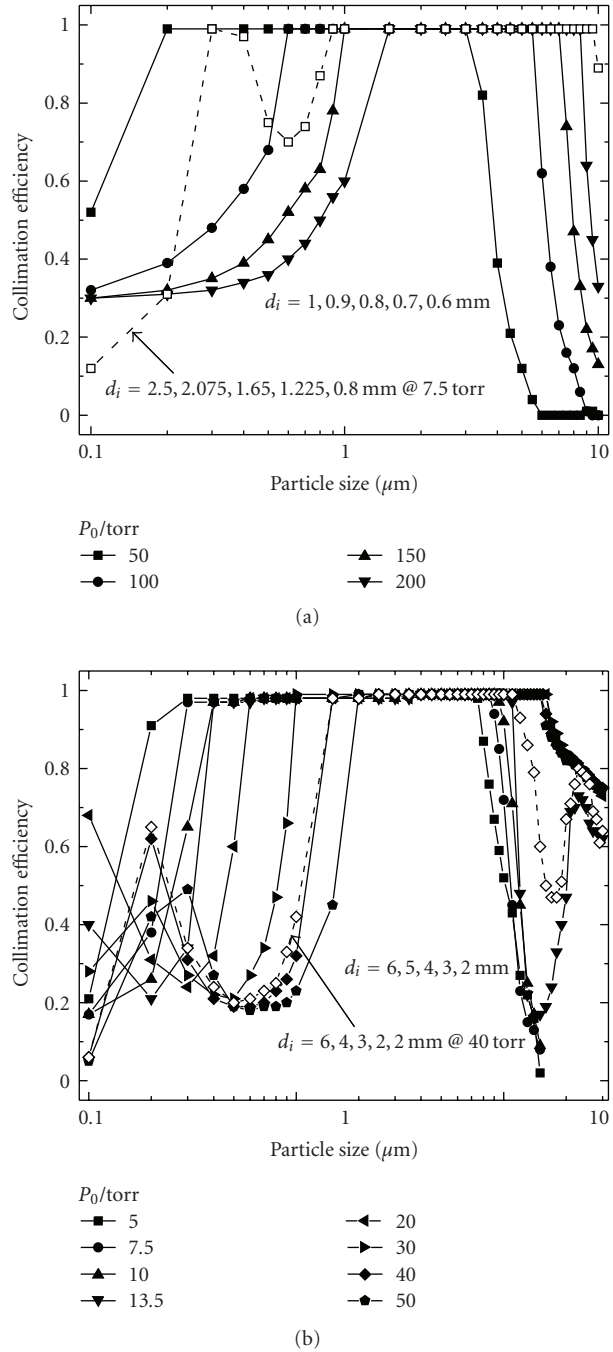

Figure 7: Dependence of the particle collimation efficiency on the operating pressure through five-lens aerodynamic inlets (D = 12 mm) ended (a) without nozzle at Q = 60 sccm and (b) with a two-stage nozzle (L_t = 10.0 mm; D_t = 2.0 mm; d_n = 1.0 mm). Note that the pressure is given in torr units here

Clearly, the size focusing range can be varied even if only the diameter of one of the lenses is changed.

Figure 7(a) presents the collimation efficiency *versus* particle size for a five-lens inlet (without terminating with an acceleration nozzle) under different pressures at a flow rate of 60 sccm. Increasing the working pressure, the smallest size in the focusing size range is increased, and so is the

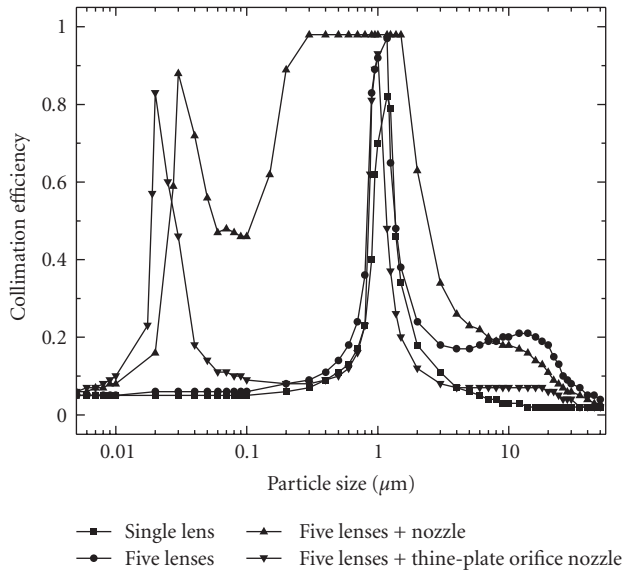

FIGURE 8: Focusing performance is compared between a thin-plate orifice and several five-lens aerodynamic inlets at $P_0 = 1000$ Pa and $Q = 60$ sccm. Inlet geometry: $D = 12$ mm; single lens ($d_i = 2.4$ mm); five lenses ($d_i = 6, 6, 2.4, 6, 6$ mm); nozzle ($L_t = 10.0$ mm, $D_t = 2.0$ mm, and $d_n = 1.0$ mm). The diameter of the thin-plate-orifice nozzle is 1.0 mm.

upper size. However, the capability of varying the focusing range by altering the upstream pressure is limited, especially at relatively high pressure. For example, particles between 0.6 and 5.5 μm can be collimated at 100 torr as shown in Figure 7(a), while only particles from 1.5 to 8.5 μm can be focused at 200 torr. Also note that both lower size and upper size limits increase with increasing pressure. Therefore, in order to extend both lower and upper size limits, the lens geometry has to be changed. As it can be seen, particles with a size range of 0.9 to 9.5 μm can be focused under a much lower pressure of 7.5 torr (cf. Figure 7(a)) for a five-lens inlet with $d_i = 2.5,\ 2.075,\ 1.65,\ 1.225$, and 0.8 mm, respectively.

When a nozzle is integrated with aerodynamic lenses, the nozzle controls the mass flow rate through the inlet. Thus, unlike in Figure 7(a), where the mass flow rate is fixed under different pressures, the flow rate through an inlet ended with a nozzle varies with the change of the upstream pressure. Figure 7(b) shows the particle collimation efficiency under different pressures for an inlet integrated with a two-stage nozzle ($L_t = 10.0$ mm; $D_t = 2.0$ mm; $d_n = 1.0$ mm). Particles are collected 5 cm away from the nozzle exit. Again, the focusing size range varies with the working pressure. It can be seen that the lower limit of the focusing range increases with the increase of pressure, while the upper size limit first increases as the pressure increases from 5 torr to 20 torr but remains almost constant at higher pressures. In other words, the upper size focusing limit reaches the plateau after 20 torr, making a further increase in pressure ineffective. In order to alter the size focusing range, the orifice geometry has to be adjusted. As shown in Figure 7(b), a different focusing range can be achieved even if only the diameter of one orifice is changed at 40 torr.

In conclusion, both orifice geometry and operating pressure play important roles in aerodynamic focusing. The effect of pressure on particle focusing diminishes at high working pressure, especially for an inlet coupled to a two-stage nozzle, but such limitation can be overcame with the use of variable orifices. Furthermore, in order to focus the same size range of particles under different pressures, or to collimate particles with different size ranges under a fixed working pressure, the lens geometry must be changed. In the analytical practice, characterization of the particle beam by mass spectrometry has to be performed at high vacuum, while the inlet is operated at medium pressure for in situ atmospheric particle sampling. As a result, a particle beam inlet with variable orifices is certainly superior to that made with fixed diameters, since particles of different desired ranges can be aerodynamically focused without the need to break the vacuum to change the inlet.

Another benefit of the variable orifice is that it can be used to selectively focus particle of a particular size. The CFD simulation results from Figure 6 indicate that an inlet with identical diameters for all five orifices can still focus particles with a small size range instead of only particles with a specific size. This is due to the fact that effective contraction factors ($|\eta_c| < 1$) are attainable for those particles slightly larger or smaller than the optimal size, thus, the overall contraction through five lenses may be strong enough for them to form a narrow beam. Therefore, the current existing five-lens inlets with either gradually reduced or identical diameters cannot be employed to focus particles of a particular size only.

We have addressed a different scheme to design a segregator to confine particles of a specific size with a five-variable-orifice inlet system. According to the previous discussion, no distinct focusing can be observed for a single lens inlet if the orifice diameter is larger than or equal to the radius of the tube diameter. So, it can be expected that a multilens inlet may be able to focus particles with the desired size *if only one orifice* is set to the required dimension, while the others are set equal to $D/2$ or larger. Figure 8 presents the comparison of the focusing performance calculated 5 cm downstream of the inlet exit for different arrangements of the inlet geometry. For a thin-plate orifice ($d_i = 2.4$ mm), about 80% of 1.2 μm particles are collimated, while almost 100% is focused with the five-lens inlet ($d_i = 6,\ 6,\ 2.4,\ 6,\ 6$ mm). By adding a two-stage nozzle ($L_t = 10.0$ mm, $D_t = 2.0$ mm, and $d_n = 1.0$ mm), particles within the range from 0.3 to 1.5 μm can be focused, and 0.03 μm particles can be also effectively concentrated on the center, with an efficiency of 88%. When a thin-plate-orifice nozzle, with a diameter of 1.0 mm, replaces the two-stage nozzle, only 0.02 (83%) and 1.0 μm (93%) particles can be efficiently collimated. From (11), it can be calculated that 1.0 μm particles are primarily focused by the aerodynamic lens with $d_i = 2.4$ mm, while 0.02 μm particles are confined by the nozzle.

Examining the detailed particle trajectories in FLUENT, a similar conclusion is obtained. Since aerodynamic focusing of nanosize (<100 nm) particles tends to be greatly affected by nonideal forces like Brownian motion [8, 11, 14–17, 24–31], such a five-lens inlet ended with a thin-plate nozzle may only focus one size particles in reality. The results suggest

that, in order to achieve size selectivity, a thin-plate-orifice nozzle rather than a two-stage nozzle should be used to accelerate the particle beam and achieve differential vacuum regions. Since the aerodynamic lens and nozzle confine different size particles, the nozzle diameter is chosen to be smaller than that of the aerodynamic lens, so that the size focused by the lens is well separated from the one by the nozzle.

5. Conclusions

In summary, focusing performance of thin-plate orifices mostly relies on the particle Stokes number, a characteristic number associated with the operating conditions as well as fluid and particle properties. For a thin-plate orifice, at a fixed mass flow rate, the optimal particle size increases with the increase of either the lens diameter or the operating pressure. However, at high working pressures, the optimal particle size is more sensitive to the variation of the lens dimensions rather than to the pressure.

It is also practicable to focus particles with a specific size using such a five-lens inlet if the orifice geometry is appropriately arranged. It is believed that the newly developed variable orifice aerodynamic inlet is theoretically superior to the one with fixed geometry, both in terms of flexibility and selectivity. Firstly, it can serve the role of a concentrator and of a segregator without complicated system modification. Secondly, the lens geometry can be easily configured to focus the same size range of particles under different working pressures. Third, its size focusing range can be dynamically changed to accommodate the needs of different applications. Clearly, a fixed geometry inlet cannot fulfill all of the above requirements.

Acknowledgment

This work was supported by DOE Grant no. DOE-DE-F602-99ER 14960.

References

[1] S. K. Friedlander, "The characterization of aerosols distributed with respect to size and chemical composition," *Journal of Aerosol Science*, vol. 1, no. 4, pp. 295–307, 1970.

[2] W. K. Murphy and G. W. Sears, "Production of particulate beams," *Journal of Applied Physics*, vol. 35, no. 6, pp. 1986–1987, 1964.

[3] G. W. Israel and S. K. Friedlander, "High-speed beams of small particles," *Journal of Colloid and Interface Science*, vol. 24, no. 3, pp. 330–337, 1967.

[4] B. E. Dahneke and Y. S. Cheng, "Properties of continuum source particle beams—I: calculation methods and results," *Journal of Aerosol Science*, vol. 10, no. 3, pp. 257–274, 1979.

[5] Y. S. Cheng and B. E. Dahneke, "Properties of continuum source particle beams—II: beams generated in capillary expansions," *Journal of Aerosol Science*, vol. 10, no. 4, pp. 363–368, 1979.

[6] N. P. Rao, J. Navascues, and J. F. de la Mora, "Aerodynamic focusing of particles in viscous jets," *Journal of Aerosol Science*, vol. 24, no. 7, pp. 879–892, 1993.

[7] J. Schreiner, U. Schild, C. Voigt, and K. Mauersberger, "Focusing of aerosols into a particle beam at pressures from 10 to 150 Torr," *Aerosol Science and Technology*, vol. 31, no. 5, pp. 373–382, 1999.

[8] H. V. Tafreshi, G. Benedek, P. Piseri, S. Vinati, E. Barborini, and P. Milani, "Aerodynamic focusing of clusters into a high intensity and low divergence supersonic beam," *European Physical Journal-Applied Physics*, vol. 16, no. 2, pp. 149–156, 2001.

[9] J. F. De la Mora and P. Riesco-Chueca, "Aerodynamic focusing of particles in a carrier gas," *Journal of Fluid Mechanics*, vol. 195, pp. 1–21, 1988.

[10] T. J. Estes, V. L. Vilker, and S. K. Friedlander, "Characteristics of a capillary-generated particle beam," *Journal of Colloid and Interface Science*, vol. 93, no. 1, pp. 84–94, 1983.

[11] R. V. Mallina, A. S. Wexler, and M. V. Johnston, "High-speed particle beam generation: simple focusing mechanisms," *Journal of Aerosol Science*, vol. 30, no. 6, pp. 719–738, 1999.

[12] P. Liu, P. J. Ziemann, D. B. Kittelson, and P. H. McMurry, "Generating particle beams of controlled dimensions and divergence—I: theory of particle motion in aerodynamic lenses and nozzle expansions," *Aerosol Science and Technology*, vol. 22, no. 3, pp. 293–313, 1995.

[13] P. Liu, P. J. Ziemann, D. B. Kittelson, and P. H. McMurry, "Generating particle beams of controlled dimensions and divergence—II: experimental evaluation of particle motion in aerodynamic lenses and nozzle expansions," *Aerosol Science and Technology*, vol. 22, no. 3, pp. 314–324, 1995.

[14] J.-W. Lee, M.-Y. Yi, and S.-M. Lee, "Inertial focusing of particles with an aerodynamic lens in the atmospheric pressure range," *Journal of Aerosol Science*, vol. 34, no. 2, pp. 211–224, 2003.

[15] X. L. Wang, F. E. Kruis, and P. H. McMurry, "Aerodynamic focusing of nanoparticles—I: guidelines for designing aerodynamic lenses for nanoparticles," *Aerosol Science and Technology*, vol. 39, no. 7, pp. 611–623, 2005.

[16] X. L. Wang, A. Gidwani, S. L. Girshick, and P. H. McMurry, "Aerodynamic focusing of nanoparticles—II: numerical simulation of particle motion through aerodynamic lenses," *Aerosol Science and Technology*, vol. 39, no. 7, pp. 624–636, 2005.

[17] X. F. Zhang, K. A. Smith, D. R. Worsnop, J. Jimenez, J. T. Jayne, and C. E. Kolb, "A numerical characterization of particle beam collimation by an aerodynamic lens-nozzle system—part I: an individual lens or nozzle," *Aerosol Science and Technology*, vol. 36, no. 5, pp. 617–631, 2002.

[18] X. Wu, N. Omenetto, B. W. Smith, and J. D. Winefordner, "Single particle fluorescence: a simple experimental approach to evaluate coincidence effects," *Applied Spectroscopy*, vol. 61, no. 7, pp. 711–718, 2007.

[19] J. Merten, N. Omenetto, X. Wu, B. W. Smith, and J. D. Winefordner, "Time and wavelength resolved laser-induced amino acid fluorescence of bacteria," submitted to *Applied Optics*.

[20] X. Wu, J. A. Merten, N. Omenetto, B. W. Smith, and J. D. Winefordner, "Development, characterization and application of a versatile single particle detection apparatus for time-integrated and time-resolved fluorescence measurements—part 2: experimental evaluation," submitted to *Laser Chemistry*.

[21] J. C. Wilson and B. Y. H. Liu, "Aerodynamic particle size measurement by laser-doppler velocimetry," *Journal of Aerosol Science*, vol. 11, no. 2, pp. 139–150, 1980.

[22] J. H. Seinfeld and S. N. Pandis, *Atmospheric Chemistry and Physics: From Air Pollution to Climate Change*, John Wiley & Sons, New York, NY, USA, 1998.

[23] M. D. Allen and O. G. Raabe, "Re-evaluation of millikan's oil drop data for the motion of small particles in air," *Journal of Aerosol Science*, vol. 13, no. 6, pp. 537–547, 1982.

[24] X. L. Wang and P. H. McMurry, "A design tool for aerodynamic lens systems," *Aerosol Science and Technology*, vol. 40, no. 5, pp. 320–334, 2006.

[25] R. V. Mallina, A. S. Wexler, and M. V. Johnston, "Particle growth in high-speed particle beam inlets," *Journal of Aerosol Science*, vol. 28, no. 2, pp. 223–238, 1997.

[26] R. V. Mallina, A. S. Wexler, K. P. Rhoads, and M. V. Johnston, "High speed particle beam generation: a dynamic focusing mechanism for selecting ultrafine particles," *Aerosol Science and Technology*, vol. 33, no. 1-2, pp. 87–104, 2000.

[27] H. V. Tafreshi, P. Piseri, E. Barborini, G. Benedek, and P. Milani, "Simulation on the effect of Brownian motion on nanoparticle trajectories in a pulsed microplasma cluster source," *Journal of Nanoparticle Research*, vol. 4, no. 6, pp. 511–524, 2002.

[28] J. Goo, "Numerical simulation of aerosol concentration at atmospheric pressure by a cascade of aerodynamic slit lenses," *Journal of Aerosol Science*, vol. 33, no. 11, pp. 1493–1507, 2002.

[29] X. F. Zhang, K. A. Smith, D. R. Worsnop, et al., "Numerical characterization of particle beam collimation—part II: integrated aerodynamic-lens-nozzle system," *Aerosol Science and Technology*, vol. 38, no. 6, pp. 619–638, 2004.

[30] A. Gidwani, *Studies of flow and particle transport in hypersonic plasma particle deposition and aerodynamic focusing*, Ph.D. thesis, Department of Mechanical Engineering, University of Minnesota, Minneapolis, Minn, USA, 2003.

[31] P. Middha and A. S. Wexler, "Particle-focusing characteristics of matched aerodynamic lenses," *Aerosol Science and Technology*, vol. 39, no. 3, pp. 222–230, 2005.